UNCLASSIFIED - UNLIMITED

(2)

NORTH ATLANTIC TREATY ORGANIZATION
DEFENCE RESEARCH GROUP

0639-90

TECHNICAL REPORT
AC/243(Panel 3)TR/6

NARSHA EXPERIMENT

Panel 3 on Physics and Electronics

RSG.12 on Maritime Remote Sensing

UNCLASSIFIED - UNLIMITED

A

UNCLASSIFIED/UNLIMITED

REPORT DOCUMENTATION PAGE

1. Recipient's Reference:	2. Further Reference:
3. Originator's Reference: AC/243(Panel 3)TR/6	4. Security Classification: UNCLASSIFIED/UNLIMITED
	5. Date: 29 OCT 90 / 6. Total Pages: 50 p.

7. Title (NU):
THE NARSHA EXPERIMENT

8. Presented at:

9. Author's/Editor's:
G.P. de Loor (*)
P.L. Lobemeier (**)

10. Author(s)/Editor(s) Address: (*) FEL-TNO, P.O. Box 96864 2509 JG The Hague, NL (**)FWG, Klausdorfer Weg 2 - 24 D-2300 Kiel 14, GE	11. NATO Staff Point of Contact: Defence Research Section NATO Headquarters B-1110 Brussels Belgium (Not a Distribution Centre)

12. Distribution Statement:

Approved for public release. Distribution of this document is unlimited, and is not controlled by NATO policies or security regulations.

13. Keywords/Descriptors:
NORMALIZED RADAR CROSS SECTION OF THE SEA, ACOUSTIC PROPAGATION, TRANSMISSION LOSS, REVERBERATION, AMBIENT NOISE, AIR-SEA INTERACTION, ATMOSPHERIC STABILITY, FRICTION VELOCITY.

14. Abstract:

Radar returns from sea surface roughness result from mechanisms which are comparable to those which generate sea state noise, absorb and scatter under water sound. It can be concluded that radar backscatter and acoustic quantities as ambient noise, reverberation, and transmission loss, are indeed related. The same experiment also shows that further data are needed to come to statistically more reliable relations. Due to the results obtained, it is clear that available models for the radar backscatter do not well apply under very stable to near neutral atmospheric conditions and therefore lead to incorrect sea surface winds under the mentionned circumstances.

UNCLASSIFIED/UNLIMITED

CONSEIL DE L'ATLANTIQUE NORD
NORTH ATLANTIC COUNCIL

UNCLASSIFIED/UNLIMITED

ORIGINAL: ENGLISH
29th October 1990

TECHNICAL REPORT
AC/243(Panel 3)TR/6

DEFENCE RESEARCH GROUP

PANEL 3 ON PHYSICS AND ELECTRONICS

Technical Report on the NARSHA Experiment

This is the technical report on the NARSHA (NATO Acoustic and Remote Sensing Shallow Water) Experiment prepared by RSG.12 on Maritime Remote Sensing under Panel 3 on Physics and Electronics. The Executive Summary of this report ("Yellow Pages") was also distributed under reference AC/243-N/305 dated 22nd June 1990.

(Signed) Dr. K.L. GARDNER
Defence Research Section

NATO,
1110 Brussels.

UNCLASSIFIED/UNLIMITED

This page has been left blank intentionally

Table of Contents

The NARSHA Experiment
Executive Summary

Summary of the Study

(i) The members of AC/243 Panel III RSG12 designed and coordinated the NARSHA (NATO Acoustic and Remote Sensing SHAllow Water) experiment which was conducted on, and in the vincinity of the German Research Platform Nordsee (FPN) in the middle of the German Bight, from 23 April to 8 May 1987. Participating nations were DK, F, GE, NL, N, UK, and US.

(ii) The primary aim of NARSHA was to investigate relationships between observations from airborne, satellite and surface radars on one hand, and acoustic observations of propagation loss, reverberation, and ambient noise on the other. Associated oceanographic parameters were measured as needed.

(iii) Radar returns from sea surface roughness result from mechanisms which are directly comparable to those which generate sea state noise, and absorb and scatter underwater sound. Remote sensing by radar offers the possibility of real time measurement of significant acoustic parameters, giving area coverage. Also, wind/wave interaction is an important element of air-sea interaction physics which is being used by several nations to develop predictive models. Such models might use remotely sensed wind and wave data as part of the required input.

(iv) Results have been published in the scientific reports listed in the bibliography and will be discussed in the present final report.

Conclusions

(v) From the NARSHA experiment it can be concluded that the radar backscatter (NRCS: Normalized Radar Cross Section) and acoustic quantities as ambient noise, reverberation loss, and transmission loss, are indeed related, but the same experiment also shows that additional data are needed to acquire statistically more reliable relations. The limited range of environmental conditions met during the experiment were such that further measurements are needed to extend the findings to more varied conditions.

(vi) These environmental conditions were very stable to near neutral. References to other data taken under the same circumstances are scarce. It is clear now, among others due to the results obtained in this experiment, that available models for the radar backscatter do not well apply to such circumstances. The reliability of the winds derived from airborne and spaceborne scatterometers - which will become a major source for wind data in the near future - depends heavily on the success of these models. Their failure demonstrates the need to circumvent them by directly relating the NRCS to the acoustic quantities of interest.

Recommendations

(vii) Further experiments connecting the NRCS with the acoustic quantities of interest are necessary to increase the statistical reliability of the relation between the two. The influence of the frequency (acoustic and radar) should be taken into account. At present three avenues to obtain the needed additional data are being pursued:

a. use of selected results from the MILOC experiment Resolute Support

b. application of results of routine measurements from FPN

c. utilisation of results expected from SAXON-FPN

After evaluation of these data sets, it will be determinde whether or not a follow-up NARSHA experiment is as well needed as promising.

(viii) Further background knowledge should be collected on the behaviour of the NRCS and the acoustic quantities of interest (with frequency as a parameter) in relation with the windvector as a function of the atmospheric stability.

Military Implications

(ix) Satellites equipped with active microwave sensors as the future European satellite ERS-1 and airborne remote sensing will increasingly become a source for environmental data. In particular, radar offers the possibility of real time survey of significant acoustic parameters, giving area coverage and so extending the range of observation.

Outline of Chapters

List of Figures

1 Objectives

1. The NARSHA (NATO Acoustic and Remote Sensing SHAllow water) experiment intended to
   - investigate and demonstrate the possibilities and advantages of using remote sensing techniques to observe and measure oceanographic surface features which can be of use in predicting acoustic quantities
   - compare and calibrate microwave systems in relation to the relevant acoustic quantities
2. The experiment was untertaken by the NATO Research Study Group: AC/243 P.03 RSG.12 "Maritime Remote Sensing". In this RSG the following nations are participating: France (F), Germany (GE), the Netherlands (NL), Norway (N), the United Kingdom (UK), and the United States of America (USA). All members contributed to this experiment. A contribution was also obtained from Denmark, although it is not a member.

2 Introduction

3. Airborne and satellite-borne remote sensing systems have the ability to make synoptic overviews of large areas of the sea surface. In such overviews environmental features become visible which are of direct importance for acoustic surveying. Radar records windspeed and -direction, sea state,directional wave spectra, currents, internal waves (as an indication of a pycnocline), bottom topography, fronts, oil patches, and shipping. The direct relation between remote sensing observations and these geophysical parameters, however, is yet far from being understood. The reaction time of remote sensing systems, with respect to changes in these parameters, is very short indicating a fairly tight relation: thus they may possibly provide even a more direct way to measure the air/sea interaction regime in the future. Satellites which will become operational in the very near future, as the European ERS-1 (1990) and the Japanese JERS (early nineties) will have radar sensors to measure the wind-vector and wave directional spectra.
4. Measurements by Farmer and Lemon [24] and more recently by Wille and Geyer [27], evaluating long-term observations, show a similar dependency on windspeed and possibly on air stability for ambient noise as found for the NRCS (Normalized Radar Cross Section) of the sea [16, 19, 20, 22].
5. Recent measurements as well from platforms [17] and from aircraft [16], however, have shown the influence of the air/sea boundary layer (air/sea temperature difference, atmospheric stability, viscosity of the water surface, etc.) on the NRCS. The empirically found relations between NRCS and the windvector at a height of 10 or 19.5 m [20, 22] therefore have a limited accuracy only. Due to this uncertainty there is a tendency to refer to 'neutral stability wind' or to the wir istress for winds derived from satellite-borne windscatterometers.
   Similar effects exist for the acoustic scattering at the sea surface, ambient noise, and propagation range. For their modelling the windspeed is used. In the future one of the major sources for the windspeed at sea will be that given by windscatterometers in satellites. This windspeed contains all the uncertainties induced by the unknown effects of the air/sea boundary layer. Theory predicts that the scattering mechanism is the same for both acoustic and radar waves. The relation between these two [illegible], may be more direct than the relation for each of them with the wind. Since windscatterometers in fact measure the NRCS of the water surface layer it seems useful to determine directly the relation between the

NRCS and the acoustic quantities mentioned and then, in the future, relate the two directly in stead of using the windvector as derived from the NRCS. In this way the effects of the boundary layer can be circumvented since in particular these effects are difficult to measure in an operational environment.

6. The work of Wille and Geyer [27] mentioned before and the more recent work of Nützel et al. [26] point in the direction of a correlation (see fig. 1). This figure gives a comparison between the acoustic (ambient noise) data and radar data and uses fig. 23 from ref. 27. The many available radar data, obtained primarily in the X- and K-band (including the SEASAT L-band data), made it possible to develop empirical models [16, 18 - 22] giving the NRCS as a function of windspeed. That is a linear relation of NRCS vs the logarithm of the windspeed. For this windspeed, however, it is often not completely clear whether it was measured at a height of 10 m or 19.5 m. We assumed 10 m for this report. Model values for three angles of radar incidence (20, 30 and 45 degr.) are introduced in fig. 1.

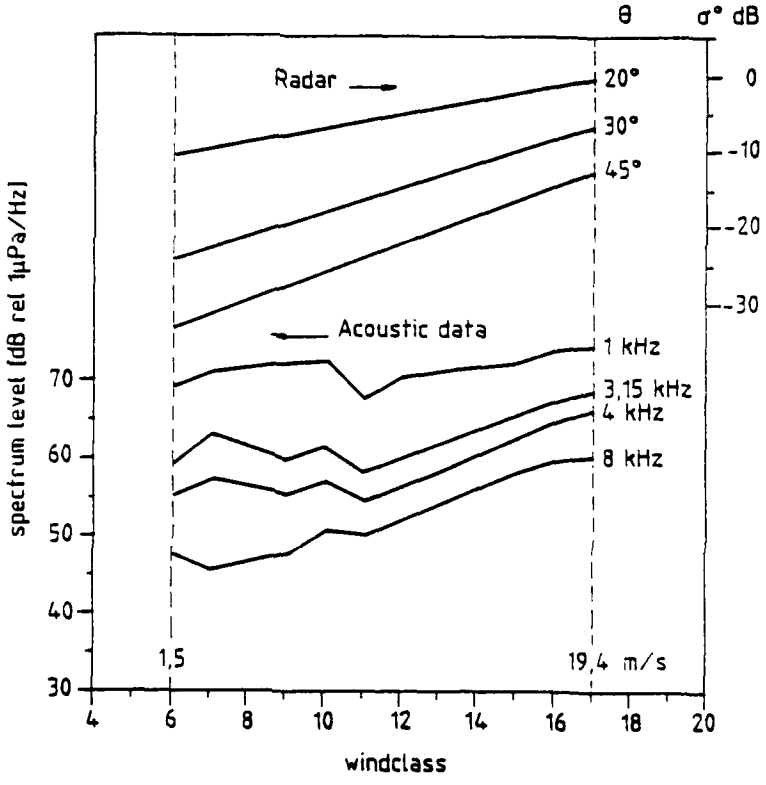

Fig 1 Comparison of radar and acoustic data (from fig. 23 of ref. 16)

7. Acoustic and radar data combined in one figure show their conformity: a similar dependency on windspeed. The NARSHA experiment was intended to investigate this correlation directly and make it explicit. The research platform NORDSEE (Forschungsplattform Nordsee, FPN, see figure 2) seemed well suited to make good measurements also in the air/sea boundary layer and so to establish the effect of this layer.

3 Experimental Set-Up

3.1 Time

8. The experiment was carried out from 22 April to 13 May, 1987. Data were collected from 27 April (Julian day 117) to 9 May (Julian day 129). During the first part of the experiment (until and including day 122 (2 May)) the weather situation was extremely stable with air-sea temperature differences often higher than 4 degrees and on occasions even going to 10 to 12 degrees. After day 122 the atmospheric situation became near neutral.

3.2 Place

9. The experiment took place at and around the German ForschungsPlattform Nordsee (FPN) in the German Bight. Figure 2 shows its position on the map. Figure 3 gives a drawing of the platform and figure 4 the ACRA-range (the ACoustic RAnge). The facilities at the platform were made available by the German Ministry of Defence.

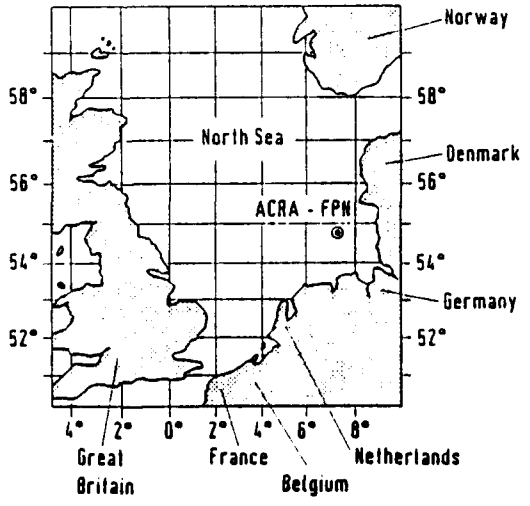

Fig. 2 Location of the German research platform Nordsee (ForschungsPlattform Nordsee, FPN)

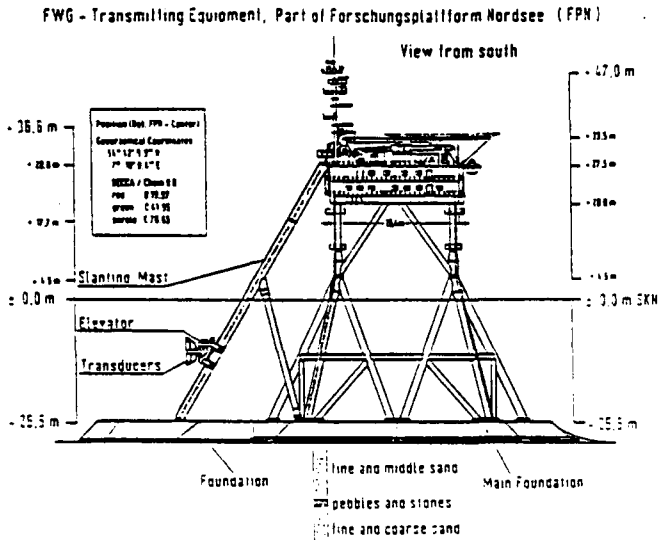

Fig. 3 The research platform FPN

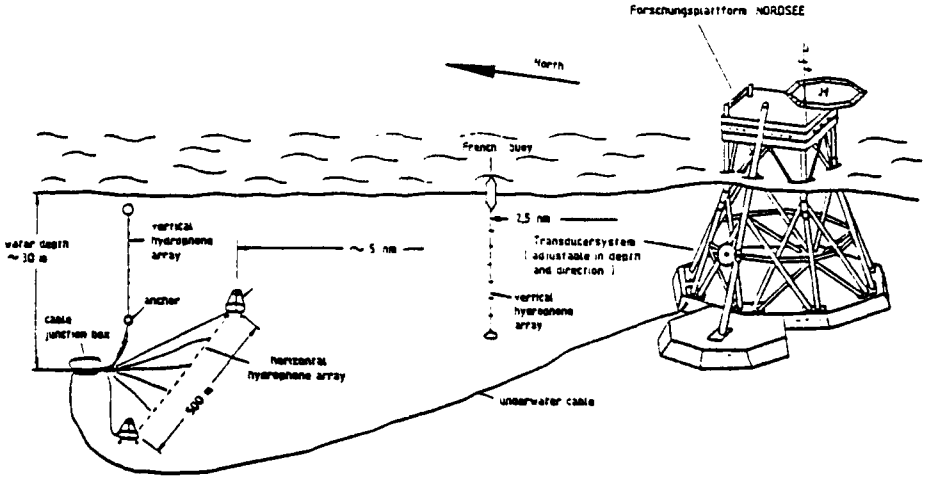

Fig. 4 The ACoustic RAnge (ACRA)

3.3 Participation

10. Below, an brief overview of the participating institutes and their activities is given.

3.3.1 Denmark

11. Department of Meteorology and Wind Energy, Risø National Laboratory:
geophysical data.
Measurement of windspeed and -direction, air temperature and the determination of the friction velocity and the drag coefficient (H = 39 m) [1, 2].

3.3.2 France

12. GERDSM: acoustic data. Ambient noise measurements in the frequency band of 50 Hz until 4 kHz were made using a buoy placed about midway the ACRA-range [3].

3.3.3 Germany

13. Germany hosted the experiment.

FWG: Coordination of the experiment.
Acoustic data using the facilities of the ACRA-range: ambient noise, propagation loss, and reverberation data at frequencies of 1 kHz, 3.15 kHz and 8 kHz were processed [7, 8, 9].
Geophysical data: windspeed and -direction at a height of 10, 5 and 4 m, friction velocity and drag coefficient (H = 5 m), and humidity profile [5, 6].

FPN: Meteorological data: Weather Log of the platform [4].

FGAN: Radar data were collected at 94 GHz with a fixed scatterometer mounted on the platform (inc. angle: 45 degr.) [10].

DLR: X-band SLAR flights on days 118 (28 April) and 119 (29 April) (report not yet submitted).

3.3.4 The Netherlands

14. FEL-TNO: Radar data.
2 X-band SLAR flights were made (4 and 6 May, Julian day 124 and 126) and a X-band ships radar (SHIRA) was placed at the platform to measure wave directional spectra [11].

3.3.5 Norway

15. NTNF: X-band Radar data. NRCS (Normalized Radar Cross-Section) data at low grazing angles (under 2 degr.) from the platform [12, 13].

3.3.6 UK

16. RAE: Satellite data. AVHRR data were supplied and SST (Sea Surface Temperature) maps around the platform [14].

3.3.7 USA

17. NRL: Radar data.
(i) Airborne/radiometric and radar measurements (13.9 GHz) along the ACRA-range and further away from the platform [15].
(ii) Measurements at K_u- and L-band with a fixed radar from the platform (incidence angle 45 degr.).

3.4 Reports

18. All nations reported separately about their activities, see ref. 1 to 15.

3.5 Data collection

19. The following data sets were collected:

3.5.1 Acoustic data

20. Ambient noise, propagation loss, reverberation (F, GE, [3, 7, 8, 9]).

3.5.2 Airborne data and radar data on FPN

21. NRCS data from the air (K_u-band, VV-polarization, and at several incidence angles between 15 and 30 degr. (USA)) [15], and X-band SLAR imagery (NL [11] and GE (DLR)).
Grounddata from the platform:
All systems were mounted about 30 m above the sea and overlooked the ACRA-range (in the 300 degr. direction).
(i) K_u- and L-band scatterometer (USA), inc. angle 45 degr.
(ii) 94 GHz scatterometer (GE), incidence angle 45 degr. [10].
(iii) X-band scatterometer (N), grazing angle under 2 degr., VV-pol. [12, 13].
Imagery: X-band ships radar (SHIRA; NL) [11].

3.5.3 Geophysical data

22. FPN: Standard meteorological data (weather log), wind speed and -direction (H = 47 m), wave height and period, air temperature (H = 33 m) and water temperature (H = -4.5 and -19 m), humidity (%), pressure, visibility, and cloudiness [4], e.g. see fig. 5

23. Special data by
FWG: Windspeed at 10, 5, and 4 m, humidity profile, friction velocity and drag coefficient (H = 5 m) [5, 6].
Risø Lab.: Windspeed and -direction, air temperature, friction velocity and drag coefficient (all at H = 39 m) [1, 2].
NRL: Radiometric data. SST (Sea Surface Temperature) was measured during sorties [15].
RAE: AVHRR data were provided for days 117, 126 and 127 [14].

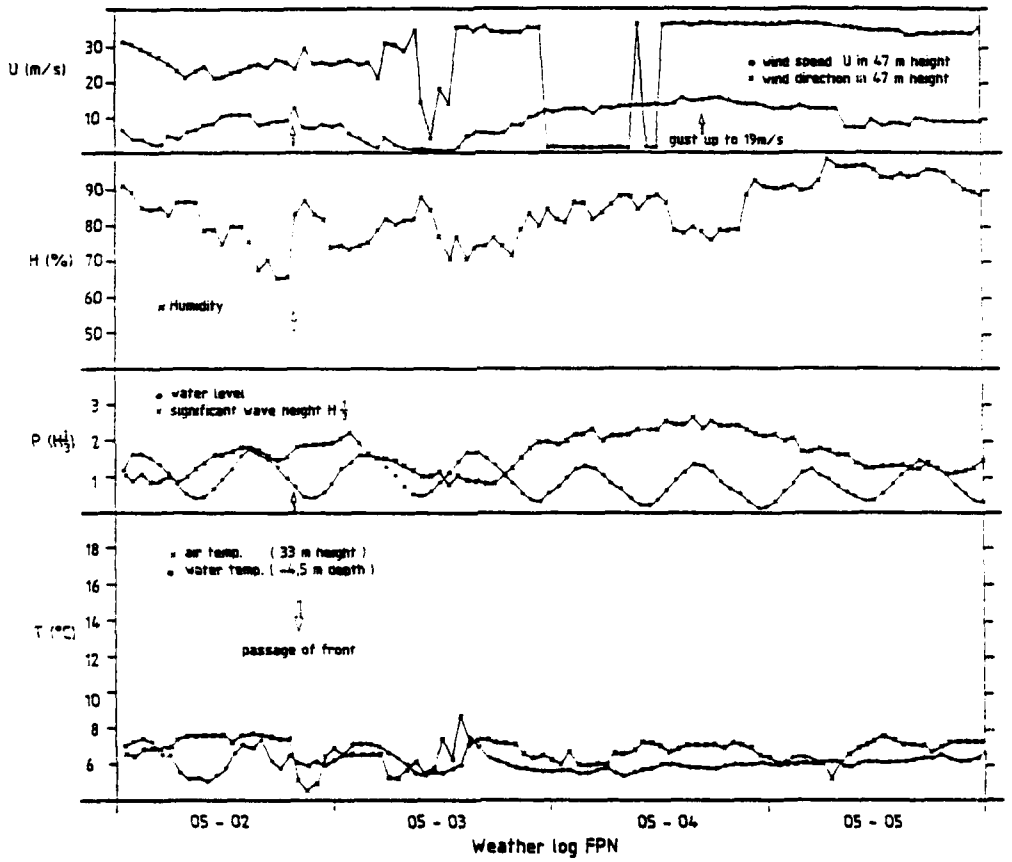

Fig. 5 Standard meteorological data (FPN weather log) from 2 May 87 until 5 May 87

4 Obtained Results

4.1 Inventory and validation

4.1.1 Acoustic data

24. The measured acoustic data were compared with the data as obtained by Wille and Geyer [27]. In their paper figure 23 is representative for the environmental situation met in this experiment. When plotting the ambient noise data as obtained in this experiment in their figure (see fig. 6) it is seen that the data fall in the expected ranges. For the 1 kHz data no dependence on wind can be seen and the data scatter as seen in figure 6. For the 4 and 8 kHz data curves can be drawn through the data which also fit well in the data set of Wille and Geyer [27] (fig. 6).

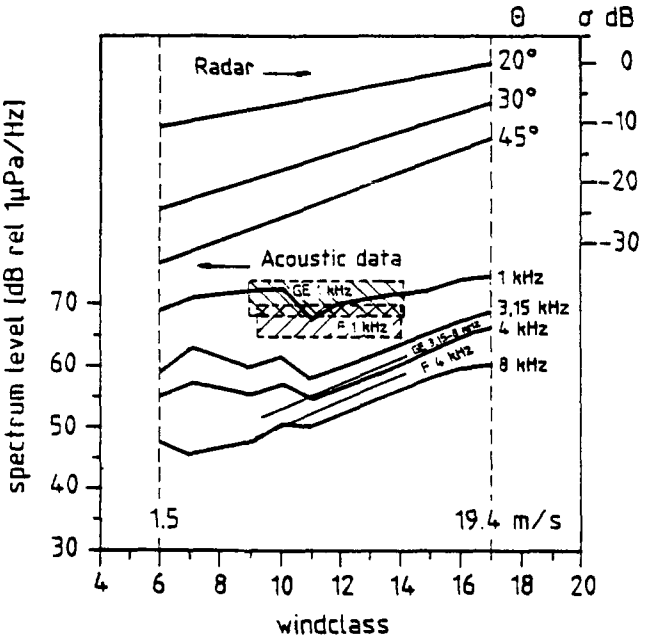

Fig. 6 Comparison of the acoustic data (ambient noise) obtained during the NARSHA experiment with the Wille-Geyer data (ref. 27)

4.1.2 Radar data

25. Many NRCS measurements have been made over the sea in the last 10 to 15 years. In particular the flight by the SEASAT and the coming of the ERS-1 satellite have brought summaries of these data sets and the development of models [16, 18 - 22]. Although there may be some problems with those models for very stable conditions [17] we still have used them here [18] to validate the radar data. All radar data were therefore plotted versus the windspeed at H = 10 m (as measured by FWG

[5]). The results are given in the figures 7 to 9. In these figures the open symbols apply to data taken on the days with very stable conditions, the closed ones to near neutral conditions (the second half of the experiment). For the FGAN data we applied the K-band model although this is incorrect. But it at least gives an impression of the trend the data should follow.

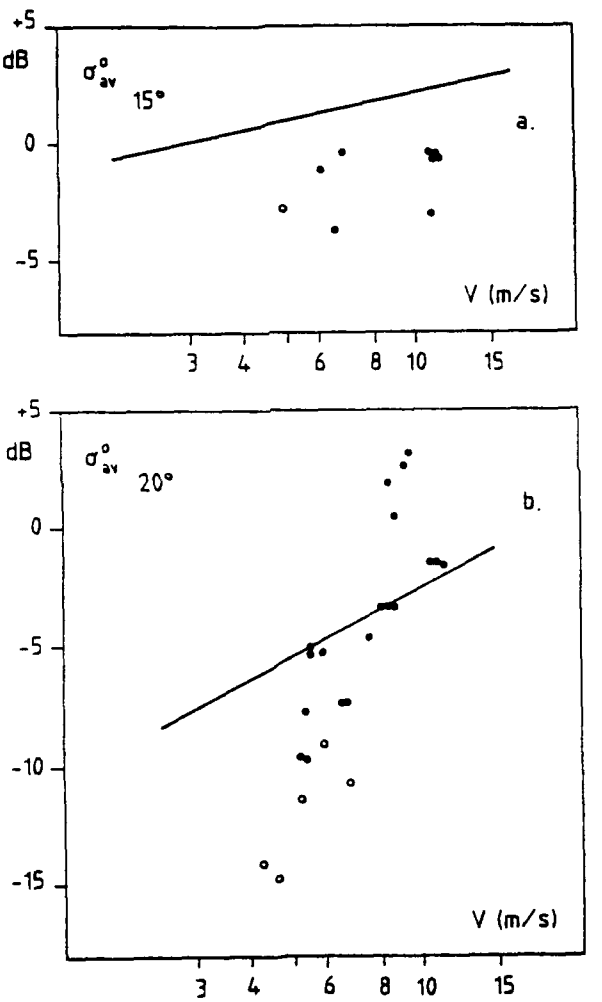

Fig. 7 NRCS σ^0 vs wind velocity V (H = 10 m).
NRL data (airborne) near FPN, 4 incidence angles.
(Lines predicted by FEL-TNO model)
○ stable, ● neutral atmospheric conditions
a: angle 15°, b: angle 20°

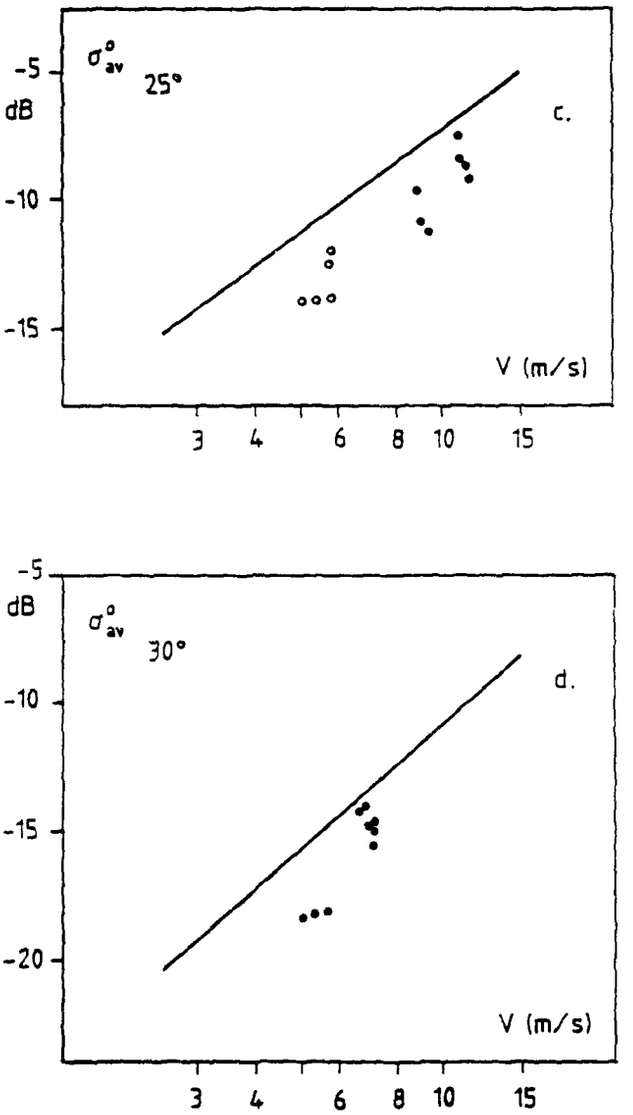

Fig. 7 NRCS σ^o vs wind velocity V (H = 10 m).
NRL data (airborne) near FPN, 4 incidence angles.
(Lines predicted by FEL-TNO model)
o stable, • neutral atmospheric conditions
c: angle 25°, d: angle 30°

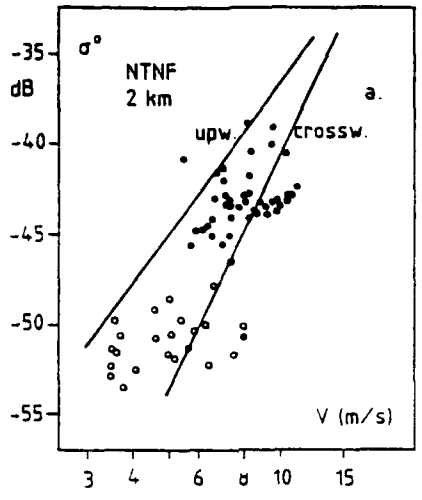

Fig. 8 NRSC σ° vs wind speed V (H = 10 m). NTNF data measured at 2 km distance from FPN, grazing angle 0.86°.
o stable, • neutral atmospheric conditions.
(Lines predicted by Sittrop's model [21])

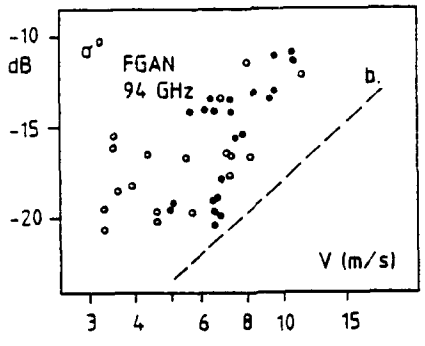

Fig. 9 NRCS σ° vs wind speed V (H = 10 m). FGAN data, 94 GHz.
o stable, • neutral atmospheric conditions.
(Lines predicted by K-band model, FEL-TNO)

26. Figure 10 shows the NRCS as measured in the K-band at vertical polarisation by NRL. These data were provided on floppy disk. The data are plotted versus this windspeed as measured at FPN and recorded simultaneously with the scatterometer data by NRL. Deviations from the model are observed for the days with stable conditions. This is to be expected and was also noted by NRL in former experiments [17].

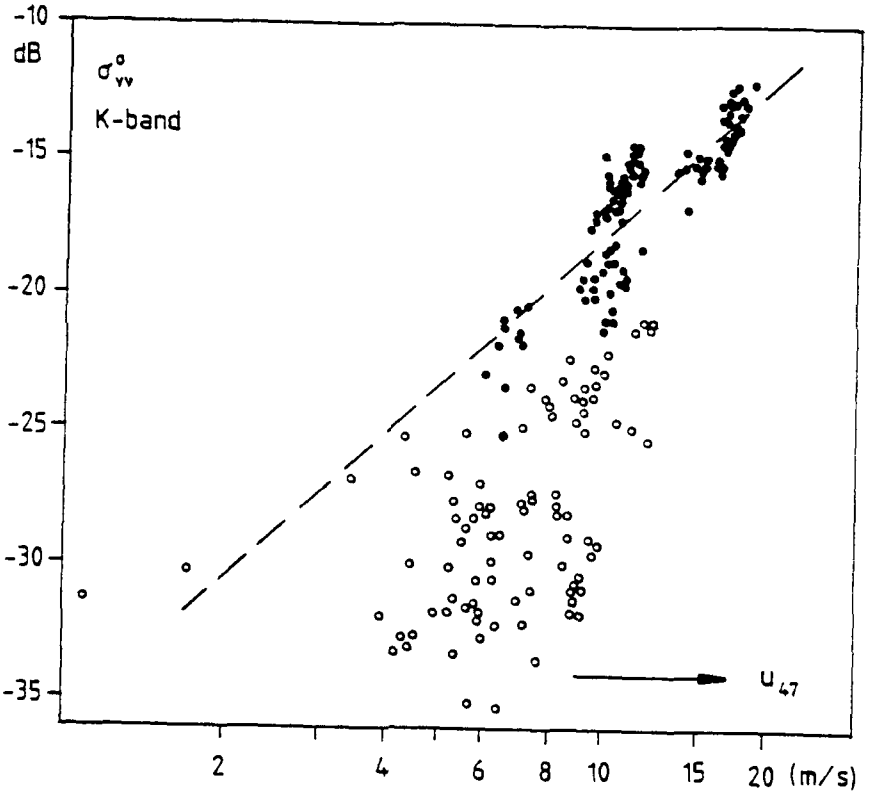

Fig. 10 NRCS σ^o vs wind speed U (H = 47 m, FPN).
NRL data taken from FPN, $\theta = 45^o$, VV-polarisation.
o stable, • neutral atmospheric conditions.
(Line is predicted by FEL-TNO model)

27. Looking through the figures 7 - 10 we see that most data fit the model reasonably well, also considering that the model applied is good only for the averaged NRCS and so does not take into account the wind direction. Only for the airborne NRL data taken at an incidence angle of 20 degr. there is an unexpected deviation, which also does not fit the general trend (of the exponent of the lines of NRCS in dB vs. the logarithm of the windspeed). The FGAN data on day 126 and 127 also show deviations from the expected behaviour.

28. With the NTNF data [12, 13] (taken at very low grazing angles, namely under 2 degr.) the model developed by Sittrop [21] was used. The data fit this model reasonably well (fig. 8) considering that stability was not taken into account.
The two SLAR flights made by NL on days 125 and 127 [11] showed a homogeneous sea surface along the ACRA range. On day 125 a ships track (midway the range) and an internal wave (at one third of the range) were visible. The associated variations in radar backscatter are small and in the same order as for ordinary sea waves. The SLAR flights carried out by GE showed slicks on day 118 at the far end of the range, between the marker buoys of the ACRA field, and in the near vicinity of the FPN.

4.1.3 Comparison

29. To obtain an impression of fluctuations to be expected in this experiment we also compared the different radar data as far as obtained simultaneously. In the figures 11 to 13 the results are plotted. The dotted lines give the expected trends predicted by the models. The spread around this line is fairly large.

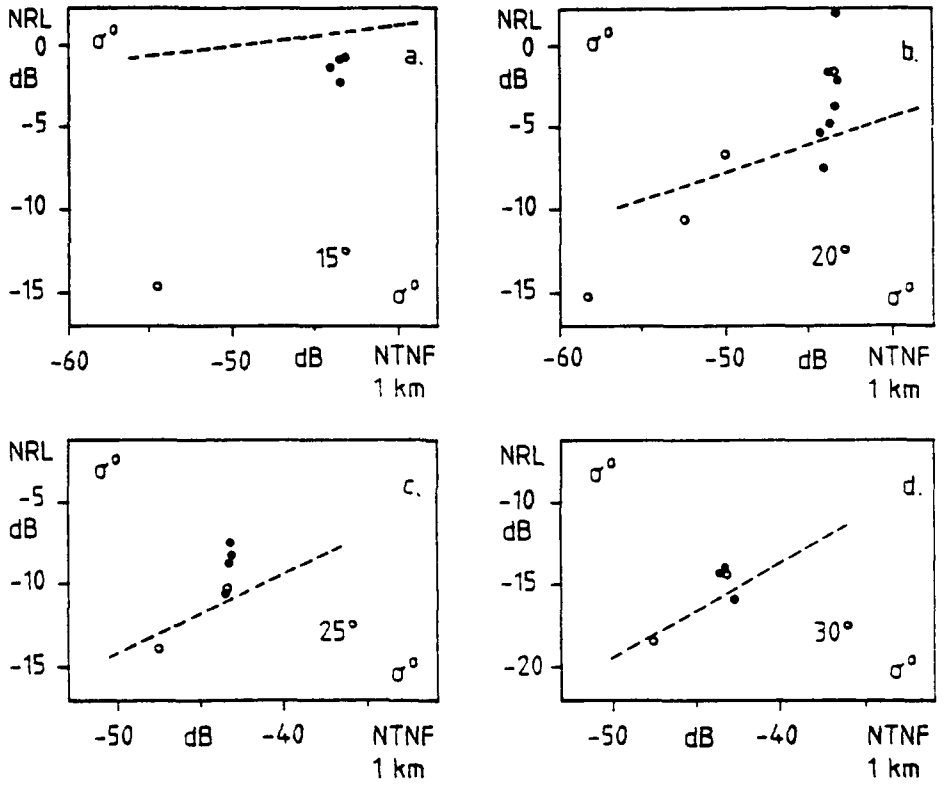

Fig. 11 NRCS σ^o as measured by NRL (airborne data) compared with the data taken simultaneously by NTNF at 1 km distance from the FPN.
o, • neutral atmospheric conditions
different NRL radar incidence angles
a: 15°, b: 20°, c: 25°, d: 30°
(Dotted line is predicted by FEL-TNO model)

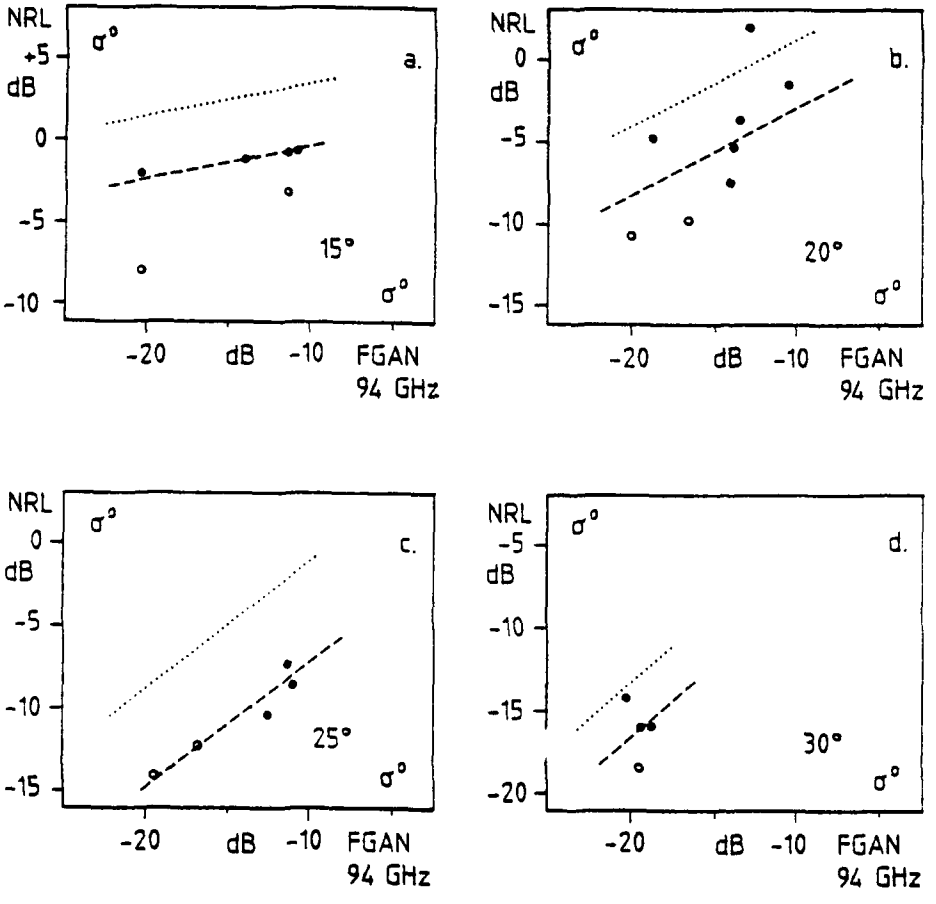

Fig. 12 NRCS σ° as measured by NRL (K_u-band airborne data)
compared with the data taken simultaneously by FGAN, 94 GHz at angle of 45°
o stable, • neutral atmospheric conditions
different NRL radar incidence angles
a: 15°, b: 20°, c: 25°, d: 30°
(Dotted line is predicted by FEL-TNO model)

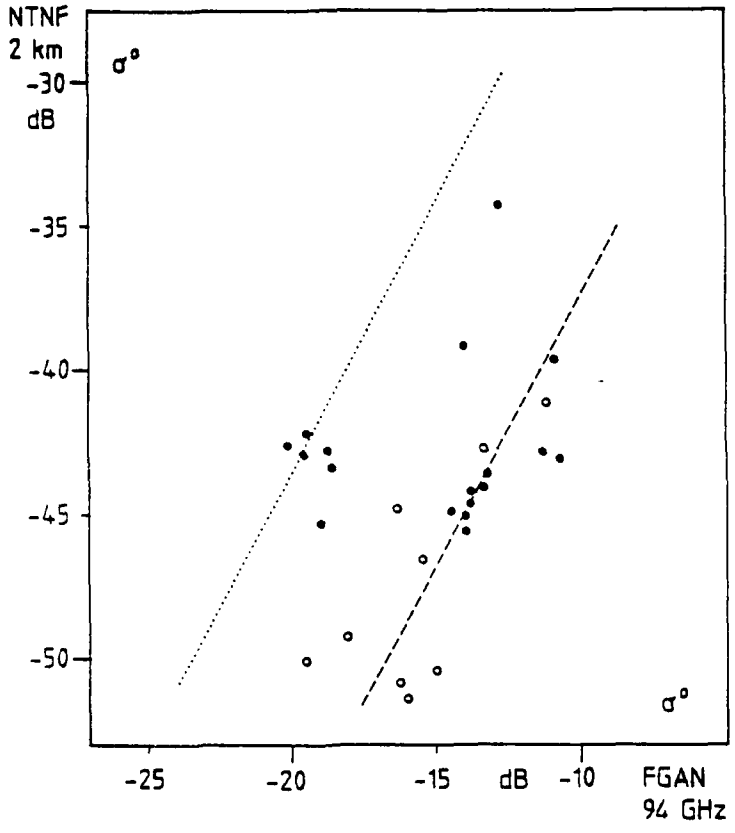

Fig. 13 NRCS σ^o as measured by NTNF compared with the data taken simultaneously by FGAN.
o stable, • neutral atmospheric conditions
(Dotted line is predicted by K-band model)

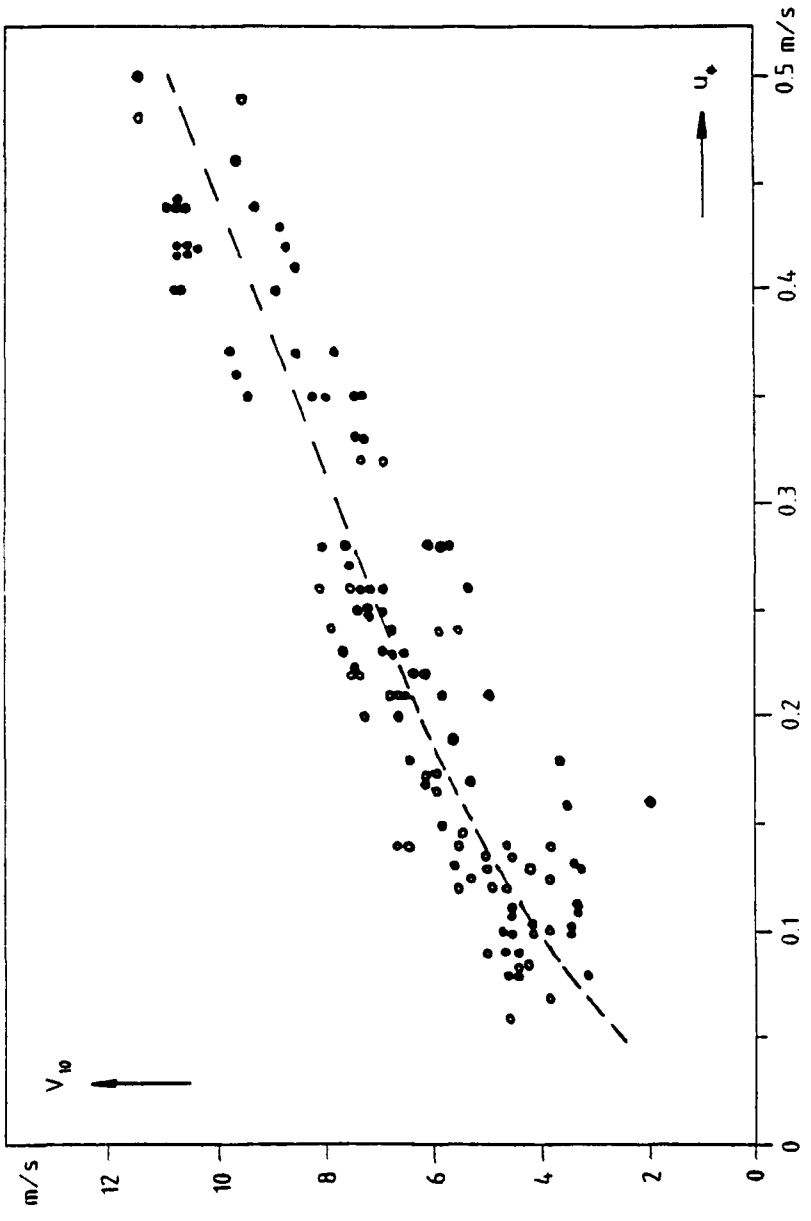

Fig. 14 Friction velocity vs wind speed (H = 10 m)
o stable, • neutral atmospheric conditions

4.1.4 Radiometric data

30. Radiometrically measured sea surface temperatures (SST) were available from the US data sets [15] (airborne data) and the AVHRR data [14]. Table 1 summarizes these data and compares SST with the bucket temperature as measured at FPN [4]. SST values and AVHRR data are not atmospherically corrected. In table 1 averages per sortie are given for the US data, where the time of overpass is provided for the AVHRR data.

day	time (GMT)	SST degr. C US	AVHRR	FPN temp. sea	air
117	11.14 - 13.39	7.1		4.8	6.8
118	13.24		2.4	4.9	10.8
119	07.21 - 08.50	6.9		6.9	9.0
120	11.07 - 14.04	10.5		5.9	11.8
124	11.03 - 14.58	6.8		5.9	6.9
125	11.17 - 13.34	4.6		6.1	7.1
126	07.12		4.6	6.4	6.8
126	11.08 - 14.05	6.8		6.5	6.8
127	08.31		5.9	7.0	6.7
127	09.45 - 13.22	7.8		7.1	6.8

Table 1: Radiometrically measured SST [14, 15] compared with the bucket and air temperatures as measured at FPN [4]

4.2 Evaluation

4.2.1 Geophysical data

31. Assuming the friction velocity u_* to be a more basic quantity than the wind speed for which the proper height to measure (H = 10 m or 19.5 m) is always discussed, all data were related to the friction velocity u_*. Therefore first the wind speed measured at 10 m (FWG, [5]) was related to the friction velocity. For the determination of this friction velocity u_* the following procedure was used. Values determined by FWG (H = 5 m, from $\sqrt{-\overline{TI}}$ [5]), by Risø (H = 39 m [1]), and those derived from the meteorological data [4, 5] by calculation, using Ezraty's model [23], were available. In case of differences between the values so obtained the greatest emphasis was put on the FWG data [5], followed by the Risø data [1] and last the calculated data [23]. On some occasions (in particular day 126) more than one data set was available, and we chose the FWG data because they were taken closer to the sea surface. This results in figure 14.

4.2.2 Acoustic data

32. Figures 15, 16, and 17 give ambient noise data plotted vs. u_*, the friction velocity. No relation is seen for the 1 kHz data: they just scatter. For 3.15, 4, and 8 kHz, however, a linear function is observed with increasing accuracy (and inclination) with the logarithm of the friction velocity u_*.
Note in figure 15 (ambient noise vs friction velocity) that the data at 3.15 kHz measured by the acoustic array at the far end of the ACRA- range interlace the 8 kHz values measured at FPN.

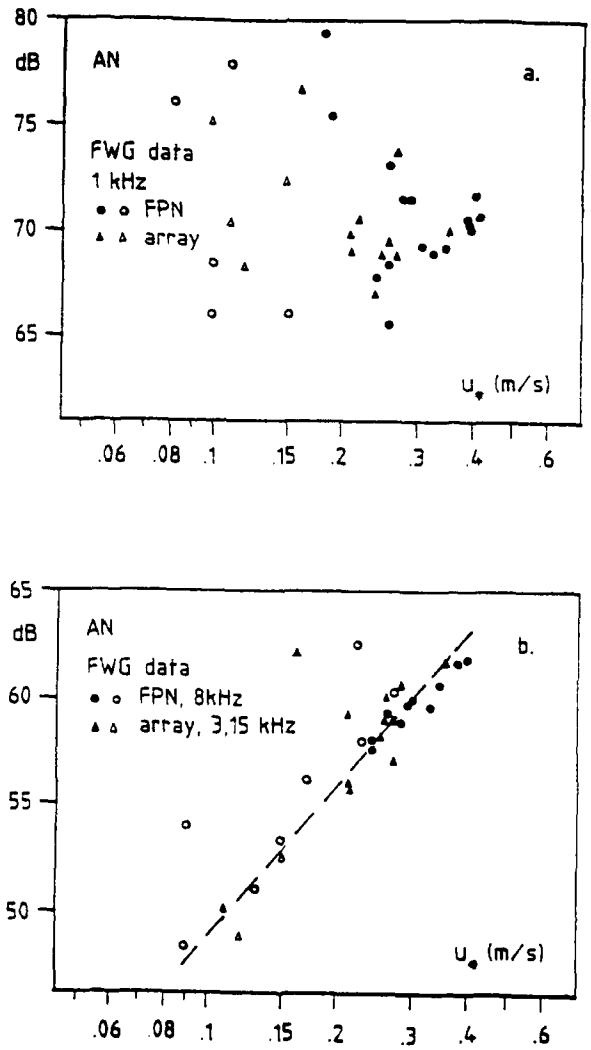

Fig. 15 Ambient noise at 1 kHz and 8 kHz vs friction velocity.
FWG data
Open symbols for data during stable, filled symbols for data during neutral atmospheric conditions

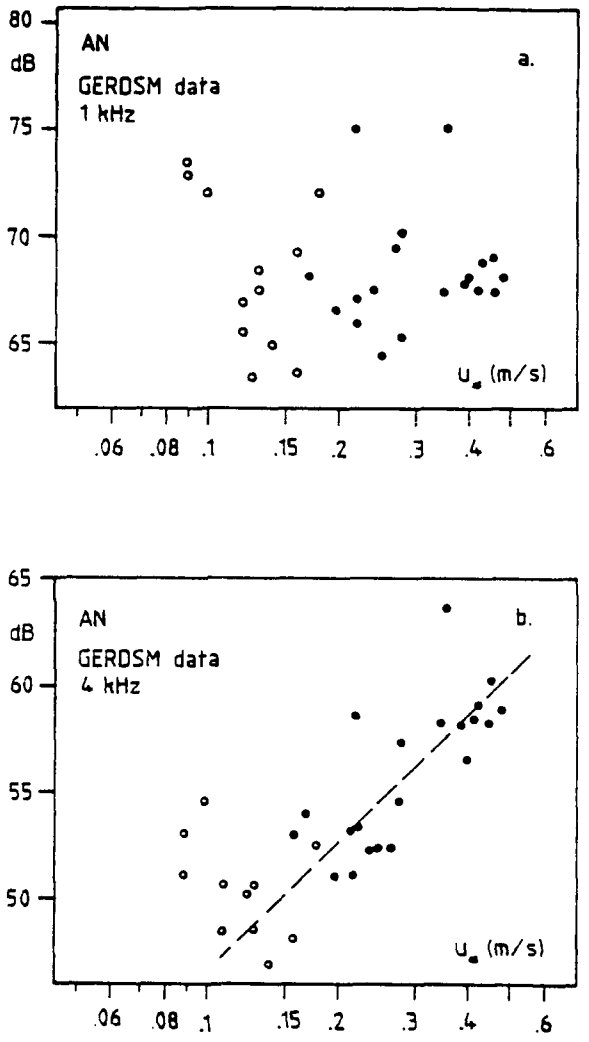

Fig. 16 Ambient noise at 1 kHz and 4 kHz vs friction velocity.
GERDSM data.
Open symbols for data during stable, filled symbols for data during neutral atmospheric conditions.

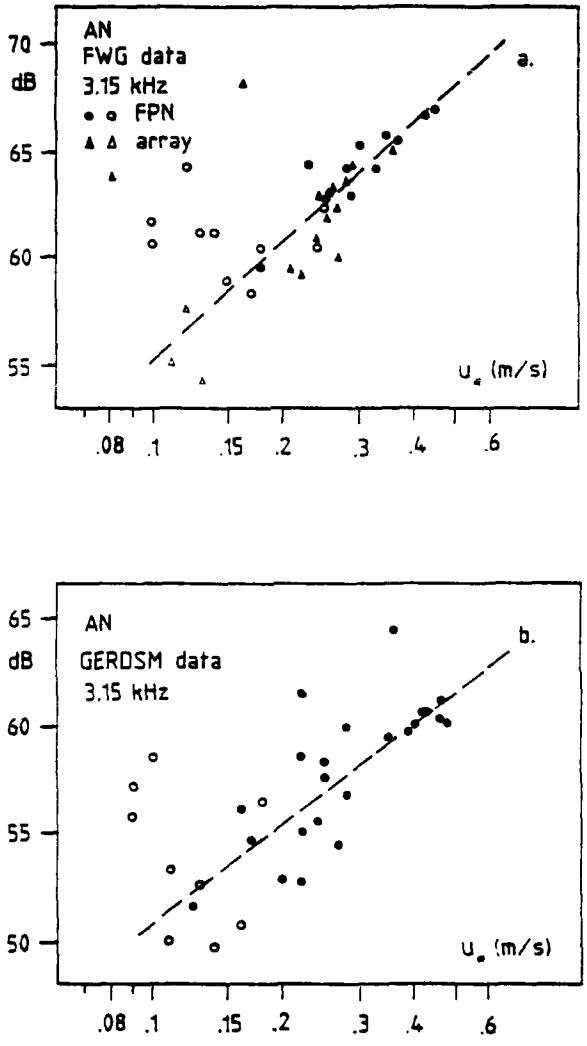

Fig. 17 Ambient noise at 3.15 kHz vs friction velocity.
GERDSM and FWG data.
Open symbols for data during stable, filled symbols for data during neutral conditions.

33. Fig. 18 (fig. 3 of ref. 27) presents the relation between transmission loss at 3.15 kHz and the wind velocity measured at 47 m height. In the low wind regime up to about 10 m/s the dependency of the transmission loss on the wind velocity seems to be week, but changes rapidly thereafter. Plots of the transmission loss (spectrum level [dB rel 1uPa/Hz]) versus the friction velocity u_* show the relation between both quantities at acoustic frequencies of 1 kHz and 3.15 kHz (fig. 19). A similar relation as in fig. 18 is observed for the transmission loss at 1 kHz, whereas the data at 3.15 kHz seem to relate the spectrum level to the friction velocity linearly. Especially in the low wind regime the friction velocity appears to describe the transmission loss better than the wind at 47 m. Due to the few data available a statistically reliable fit cannot be given.

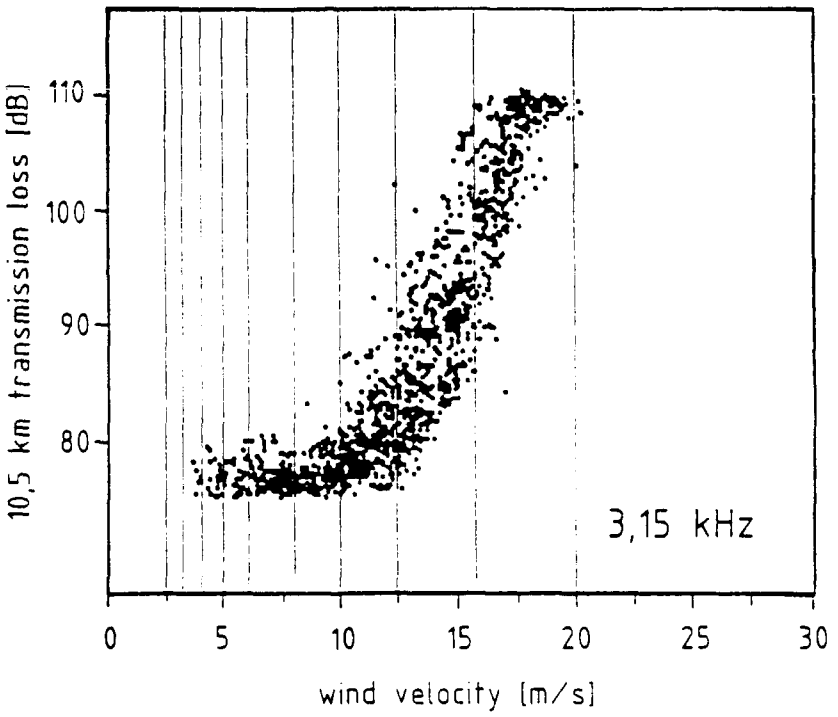

Fig. 18 Transmission loss at 3.15 kHz vs wind velocity (H = 47 m) acc. to ref. 25 (fig. 3, p. 298)

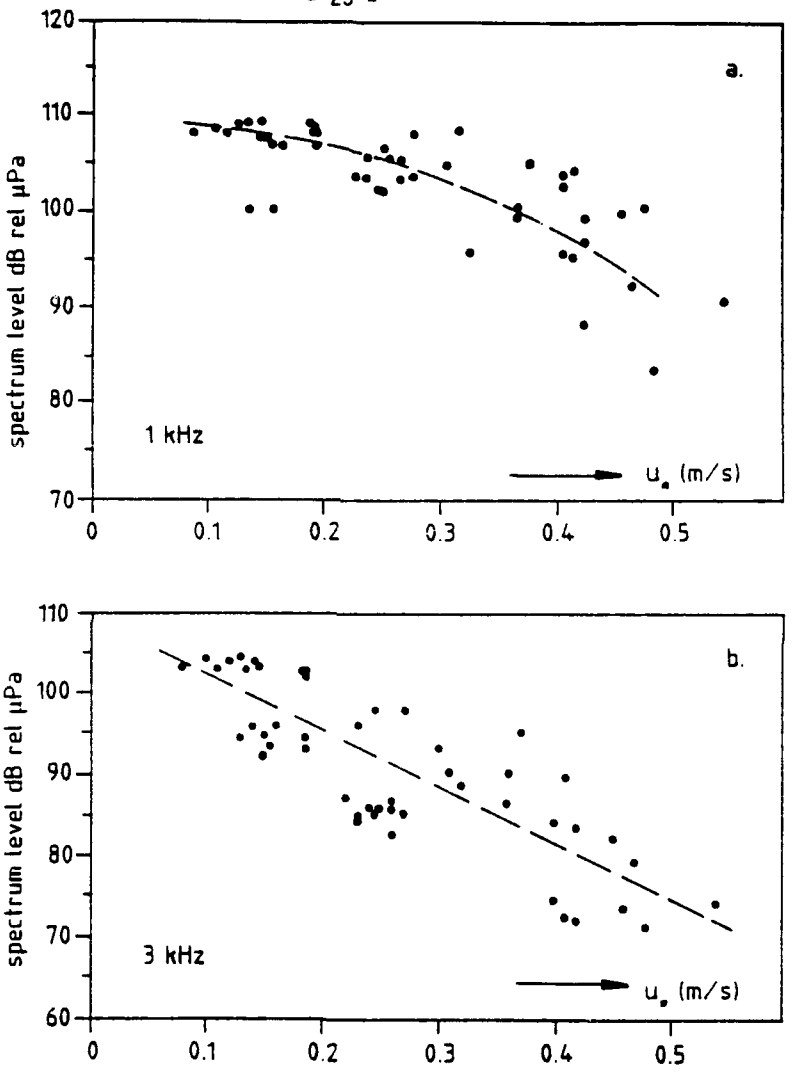

Fig. 19 Transmission loss at 1 kHz and 3.15 kHz vs friction velocity. FWG data. (The spectrum level [dB rel 1 μPa/Hz] is given for the Transmission Level (TL); TL = Source Level (SL) - Spectrum Level
1 kHz: SL = 190.75 dB rel 1 μ Pa/Hz
3.15 kHz: SL = 202.50 dB rel 1 μ Pa/Hz)

4.2.3 Radar data

34. Also the radar data were plotted as a function of the friction velocity u_*. See the figures 20 to 23.

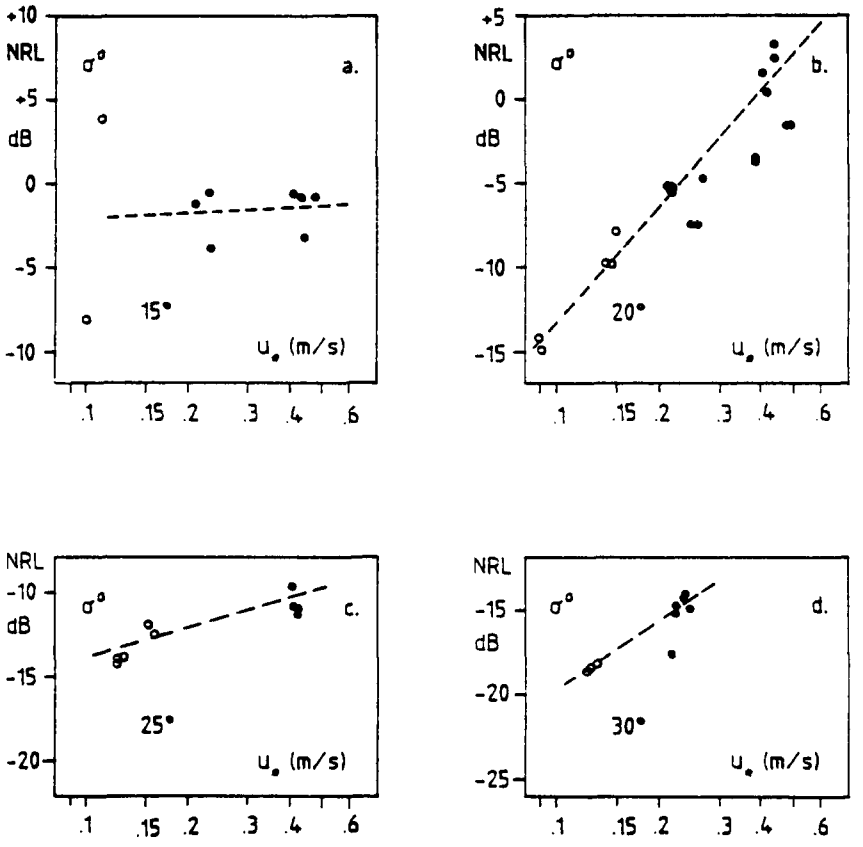

Fig. 20 NRCS σ^o vs friction velocity. NRL airborne data measured near FPN for different radar incidence angles a: 15°, b: 20°, c: 25°, d: 30°

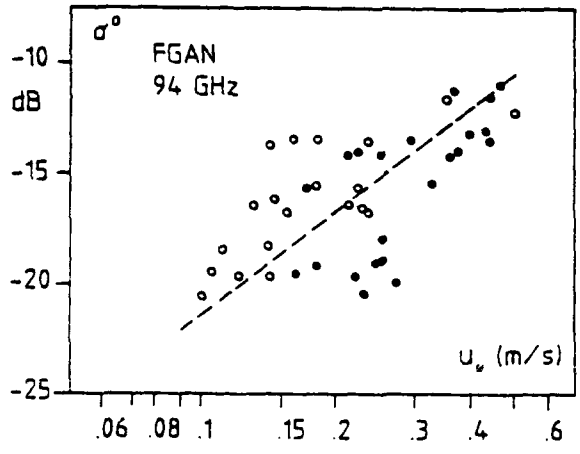

Fig. 21 NRCS σ^0 vs friction velocity.
FGAN 94 GHz data
○ stable, • neutral atmospheric conditions

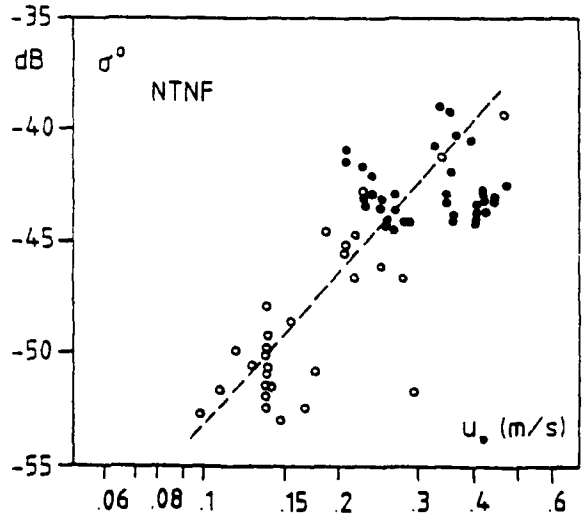

Fig. 22 NRCS σ^0 vs friction velocity.
NTNF data
○ stable, • neutral atmospheric conditions.

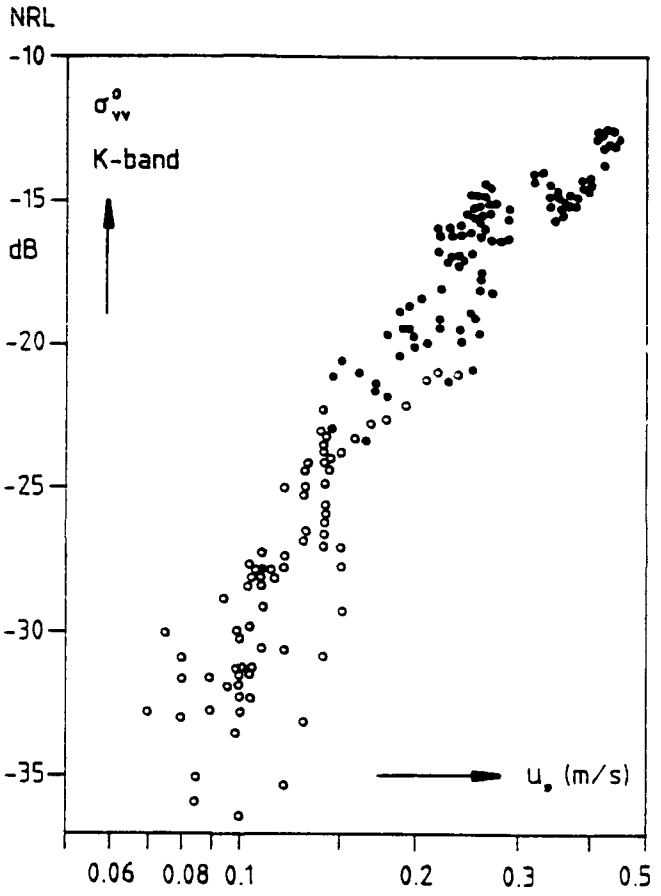

Fig. 23 NRCS σ^o vs friction velocity.
NRL data (FPN)
o stable, • neutral atmospheric conditions

4.2.4 Acoustic data versus radar data

35. When plotting the acoustic data versus the radar data taken simultaneously we met a problem. There were too few acoustic data for a statistically reliable fit with all the NRL airborne data. When all airborne data had been taken at one fixed angle only, this problem could possibly have been avoided, but now no statistically reliable conclusions can be drawn from these excellent data sets, since there are too few measurements per incidence angle.

36. In the figures 24 to 27 the ambient noise data are compared with the other radar data. In the figures also the expected relations are given (broken lines). A large spread in the data is observed. When we exclude day 126 and 127 from the FGAN data a better fit is obtained. Comparing the spread in the data with those relating the radar data mutually (figures 11 to 13), however, we see that this spread is similar in magnitude.

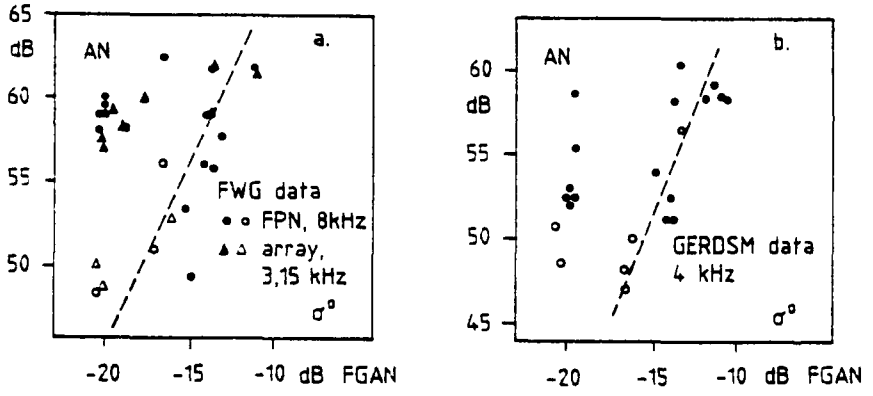

Fig. 24 Ambient noise data vs FGAN radar data taken simultaneously
○ stable, • unstable atmospheric conditions

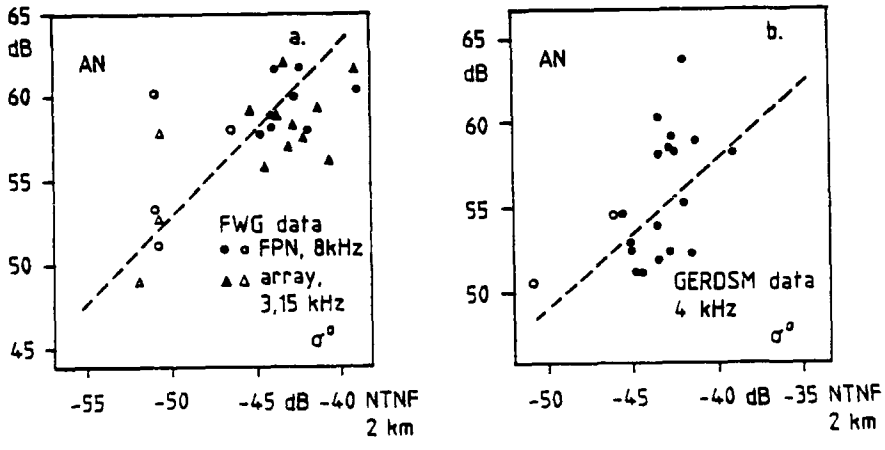

Fig. 25 Ambient noise data vs NTNF data taken simultaneously
○ stable, • neutral atmospheric conditions

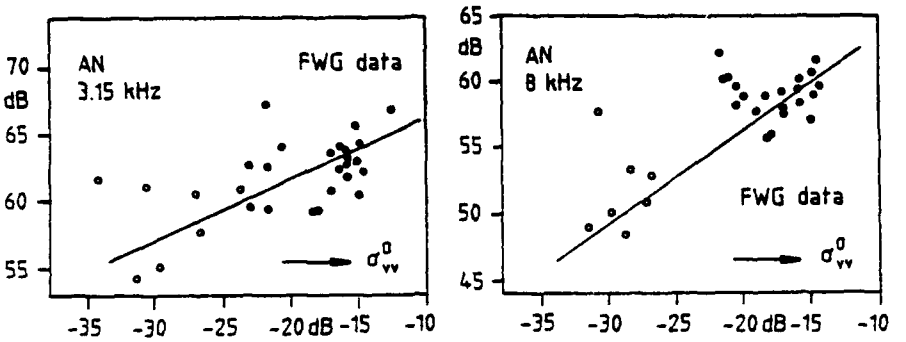

Fig. 26 Ambient noise data (FWG) vs NRL σ^0_{vv}
○ for stable, ● for neutral atmospheric conditions

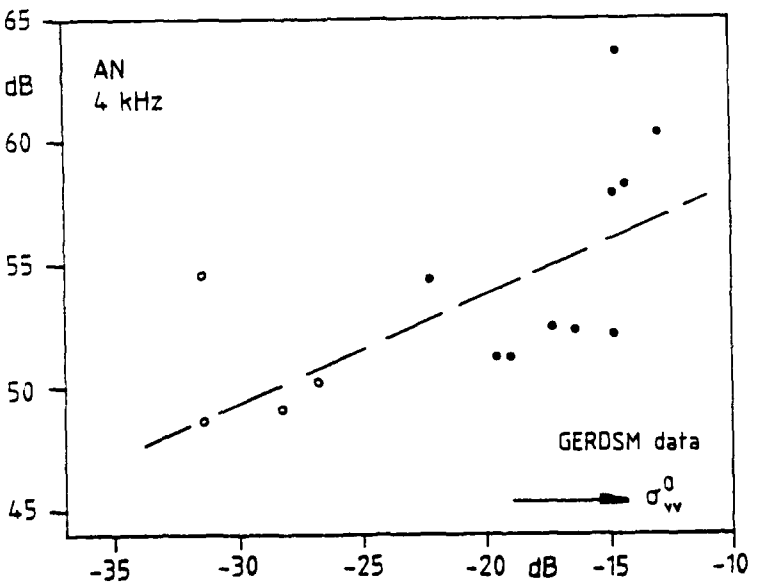

Fig. 27 Ambient noise data (GERDSM) vs NRL σ^0_{vv}
○ for stable, ● for neutral atmospheric conditions.

37. The signal level as a measure for the transmission loss, (spectrum level [dB rel 1μPA/Hz]) received by hydrophones in different depth at frequencies of 1 kHz, 3.15 kHz and 8 kHz, is plotted against the NRCS σ^o given by the W-band (94 GHz) radar (FGAN; fig. 28) and the K_u-band (13.9 GHz) radar (NRL; fig. 29). Considering that the receiving level depends on the depth of the hydrophone the scattering data of fig. 28 - spectrum level vs NRCS at 94 GHz - show the following tendency:

38. In the low wind regime (approx. $U < 8$ m/s, $\sigma^o < -14$ dB) the dependency of both quantities is weak and becomes stronger with higher wind velocity corresponding to a higher σ^o ($\sigma^o > -14$ dB).

39. The plot of the transmission loss expresses this trend weakly at 1 kHz, stronger at 3.16 kHz and 8 kHz. Going to higher acoustic frequencies the change between weak and strong dependency of the transmission loss on the NRCS σ^o seems to be shifted to lower σ^o - values, i.e. lower wind velocity. Due to the few available data, not providing accurate statistics, reliable fitting curves and values cannot be given. More investigations are neccessary.

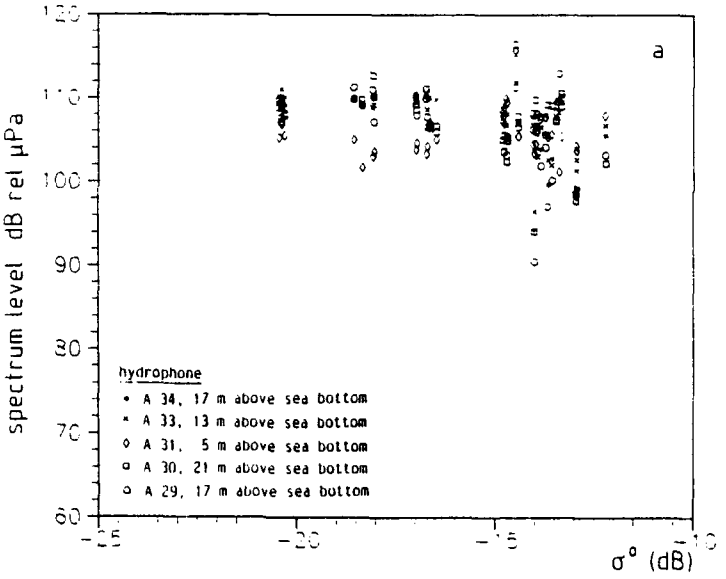

Fig. 28 Spectrum level at 1 kHz, 3.15 kHz and 8 kHz vs FGAN radar σ^o
Transmission loss = Source level (SL) - Spectrum level;
(a: 1 kHz, SL = 190.75 dB rel 1 μ Pa/Hz)

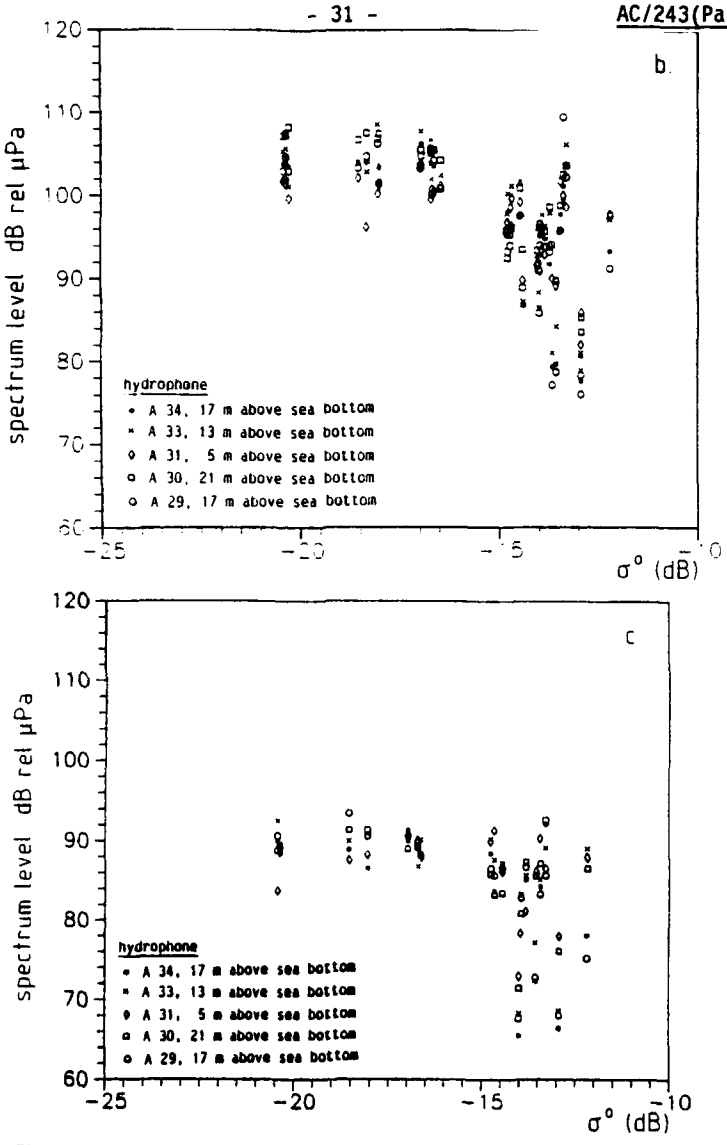

Fig. 28 Spectrum level at 1 kHz, 3.15 kHz and 8 kHz vs FGAN radar σ°
Transmission loss = Source level (SL) - Spectrum level
(b: 3.15 kHz, SL = 202.50 dB rel 1 μ Pa/Hz
c: 8 kHz, SL = 202.75 dB rel 1 μ Pa/Hz)

40. The data of fig. 29 show the relation of the acoustic spectrum level vs NRCS of the K_u-band radar (NRL). The hydrophones were deployed in different depth. The following tendency is observed:
41. In the low wind regime (approx. u ⟨ 8m/s, σ^o⟨ - 20 dB) the dependency of both quantities is weak and similar to the dependency of the spectrum level and the NRCS at 94 GHz. Even the onset of strong scattering in the acoustic level at 1 kHz is in the same NRCS range of approx. - 15 dB, the begin of more frequent wave breaking.
42. At the acoustic frequency of 3.15 kHz a first drop of the spectrum level occurs at $\sigma \approx$ -26 dB (u $\approx$ 4 m/s) - the begin of the transition zone from a viscous to a turbulent flow at the sea surface and stronger activities of 1 cm long capillary waves.
43. They act as scatterers for electromagnetic waves at 13.9 GHz. A similar behavior is found at the acoustic frequency of 8 kHz. This phenomena is not observed in the NRCS at 94 GHz. The electromagnetic wave at this frequency is scattered by capillary waves in the order of 0.1 cm wavelength, already generated by a weak breeze, i.e. the 94 GHz radar sees scatterers at very low wind speed.
44. Due to the few data available both data sets of fig. 28 and 29 cannot compared in more detail. Statistically reliable relations cannot be given.

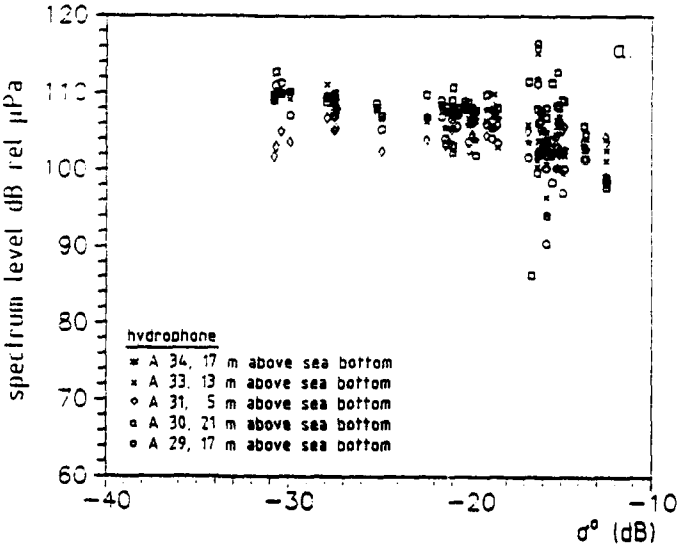

Fig. 29 Spectrum level at 1 kHz, 3.15 kHz and 8 kHz vs NRL K_u- band radar σ^o
Transmission loss = Source level (SL) - Spectrum level
(a: 1 kHz, SL = 190.75 dB rel 1μ Pa/Hz)

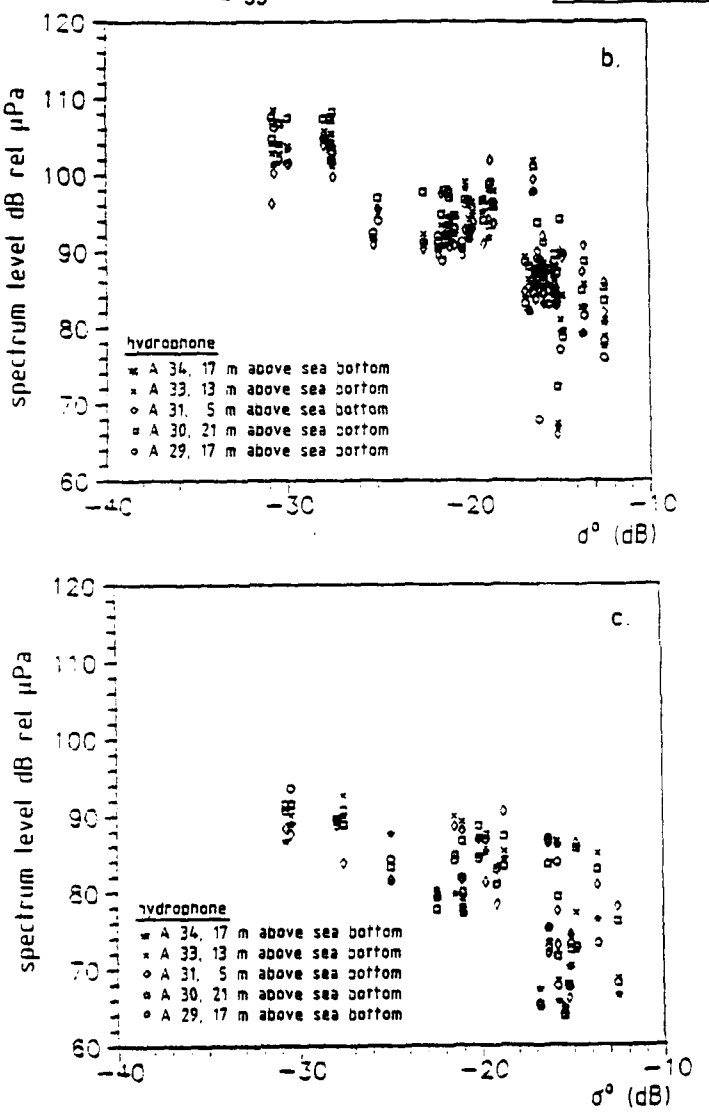

Fig. 29 Spectrum level at 1 kHz, 3.15 kHz and 8 kHz vs NRL K_u-band radar σ°
Transmission loss = Source level (SL) - Spectrum level
(b: 3.15 kHz, SL = 202.50 dB rel 1 μ Pa/Hz
c: 8 kHz, SL = 202.75 dB rel 1 μ Pa/Hz)

45. From the NARSHA report [7] the reverberation level was calculated at the frequencies of 1 kHz, 3.15 kHz and 8 kHz for 5 seconds and 10 seconds after the sound transmission (ping). The values are corrected due to instrumental characteristics of the receiving and transmitting system, i.e. the directivity index and the transmitted energy (source level/1 sec) are substracted. The corrected reverberation levels are plotted versus NRCS σ^o of the 94 GHz and the 13.9 GHz (vv-pol) radar (fig. 30). Similar tendencies are seen as in figure 28 and 29 (transmission loss versus NRCS σ^o). The plot for the 1 kHz signal shows scattering at low wind velocities; for the 3.15 kHz signal returned 5 seconds and 10 seconds after the ping the reverberation loss increases with increasing NRCS, i.e. wind velocity, beyond $\sigma^o > -15$ dB for the W-band (94 GHz, FGAN) radar, whereas beyond $\sigma^o > -21$ dB for the K_u-band (13.9 GHz, NRL) radar. The data of the signal at 8 kHz measured 5 seconds and 10 seconds after the ping scatter.

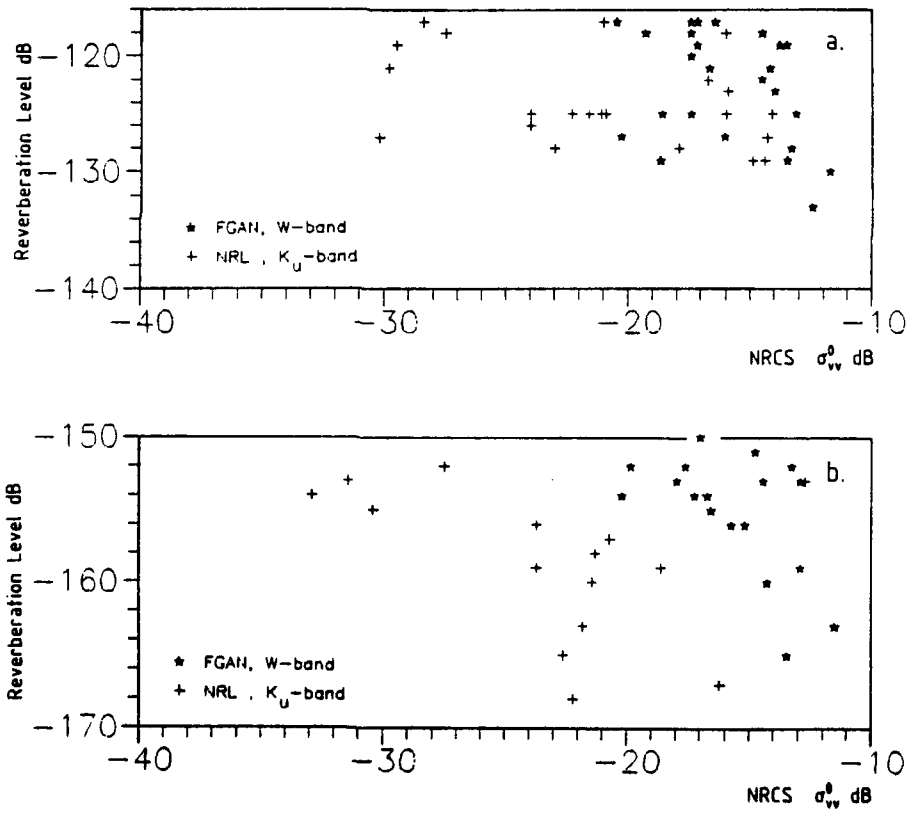

Fig. 30 Reverberation level vs NRCS, FGAN and NRL radar data taken simultaneously (a: 1 kHz/5 s, b: 3.15 kHz/10 s)

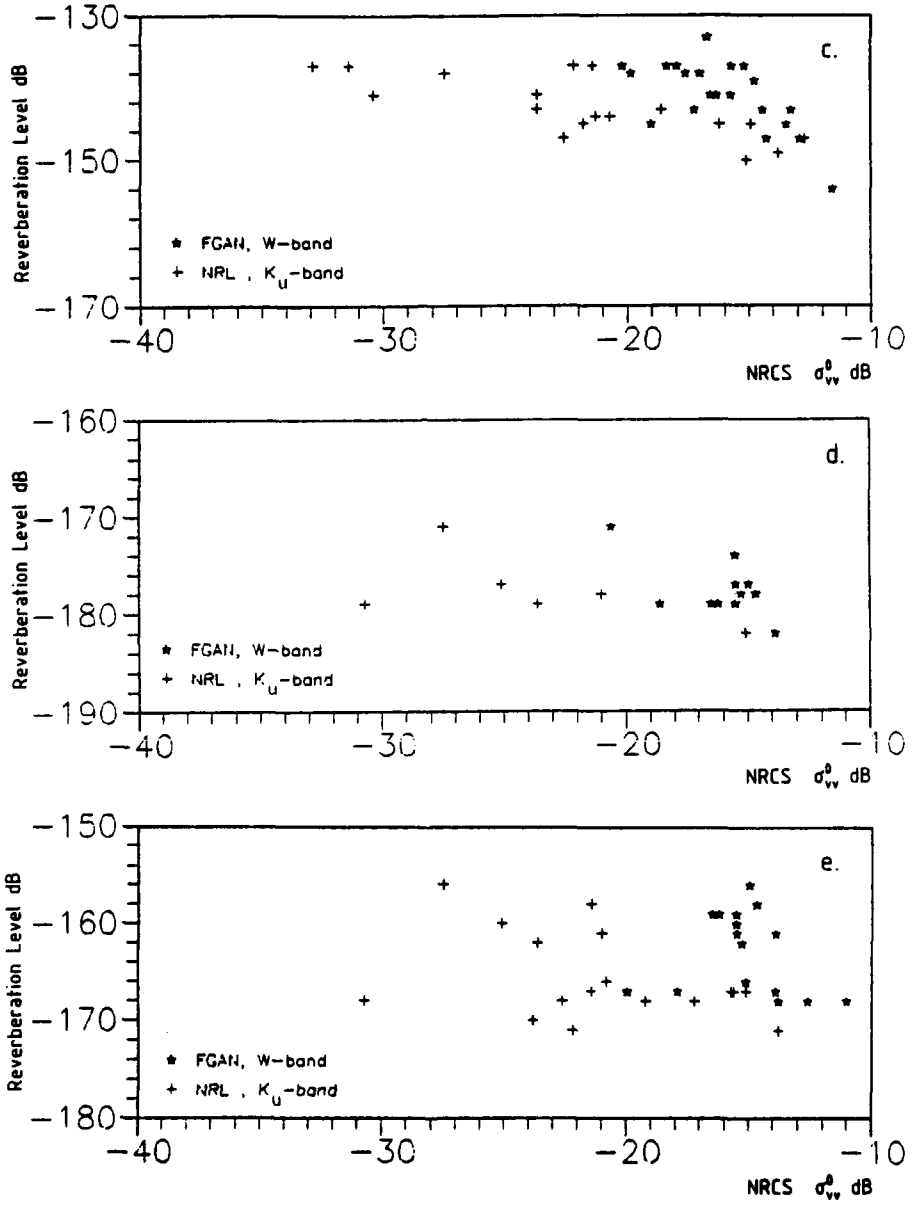

Fig. 30 Reverberation level vs NRCS. FGAN and NRL radar data taken simultaneously (c: 3.15 kHz/5 s, d: 8 kHz/10 s, e: 8 kHz/5 s)

5 Discussion and Conclusions

46. Looking at the figures 24 to 29 it can be seen that the NRCS is related with the ambient noise, the transmission loss, and the reverberation. But the same figures also show that further data are needed to achieve statistically more reliable relations. The conditions met during the experiment were such that further confirmation is necessary since the method in particular will be useful during such environmental conditions.

47. These atmospheric conditions were very stable to near neutral. Comparable data sets taken under the same circumstances are scarce. It is clear now, due to the results obtained in this experiment, that available models for the radar backscatter fail under these circumstances. The reliability of the winds derived from airborne and spaceborne scatterometers rely heavily on the success of these models. Their failure demonstrates the need to circumvent them by directly relating the NRCS to the acoustic quantities of interest. With all restrictions mentioned this NARSHA experiment now shows that the two are related directly. However, for the interpretation of all our data the environmental conditions as met also gave difficulties in their interpretation. It has been common practise to relate the acoustic and radar data to the directly measured wind speed. In this report we used the friction velocity u_* as the linking quantity between the different data sets. The conditions were such during the experiment that this velocity could not be determined accurately at all times. This again restricts the number of useful data and the possibility to give statistically reliable results. A number of scientific questions remain unanswered as e.g.:

- The actual behaviour of the NRCS under very stable conditions and the reason of its large drop when stability increases.
- The behaviour of the NRCS at 94 GHz is not well understood. For the backscatter the sea waves in resonance with the radar waves are important. In the K-band these are the waves in the transition region between gravity and capillary waves where in the W-band we are far in the capillary region (above 100 Hz) of the sea waves.
- The influence of the frequency (acoustic and radar) was not investigated. The available data sets were measured at radar wave length of 3 cm (X-band) to 3.2 mm (W-band) and compared with acoustic data at wavelength of 1,5 m (1 kHz), to 19,8 cm (8.0 kHz). Nevertheless the NARSHA results show that ambient noise, transmission loss, and reverberation are related to the NRCS measured at the high radar frequencies.
- Effects of the wind direction on the NRCS and the acoustic quantities were not investigated due to the limited number of data sets.

6 Recommendations

48. Further experiments connecting the NRCS with the acoustic quantities of interest are necessary to increase the statistical reliability of the relation between the two. The influence of the frequency (acoustic/radar) should be taken into account.

49. Further background knowledge on the behaviour of the NRCS and the acoustic quantities of interest (with frequency as a parameter) should be gathered as a function of atmospheric stability.

ANNEX I to
AC/243(Panel 3)TR/6

NARSHA Bibliography The reports are provided by the participating nations

G: Geophysical data
A: Acoustic data
R: Radar data

Denmark

[1] F.A. Hansen and S.E. Larsen: Description of data format and data quality of the meteorological data collected by Risø National Laboratory during the NARSHA experiment on the FPN platform in the spring of 1987; Report of the Department of Wind Energy, Risø National Laboratory; fall 1987. (G)

[2] F.A. Hansen and S.E. Larsen: Analysis of athmospheric turbulence data taken over the North Sea during the 1987 NARSHA experiment; Report of the Department of Wind Energy, Risø National Laboratory; 1988. (G)

France

[3] J.L. Esperandieu and M. Simon: Ambient noise measurements during NARSHA '87 (North Sea); Report no. 56983 ET/LD. GERDSM; 21 April 1988 (NATO RESTRICTED). (A)

Germany

[4] FPN Meteorological data. (G)

[5] S. Stolte: Measurements of environmental parameters during NARSHA '87; Internal FWG-Report 1988-3; 1988 (NATO RESTRICTED) (G)

[6] S. Stolte: Boundary layer parameters during NARSHA 1987, FWG-report 1989-2; 1989 (NATO RESTRICTED). (G)

[7] H. Herwig and B. Nützel: Measurements of channel reverberation during NARSHA '87; Internal FWG-report 1988-6; 1988, (NATO RESTRICTED). (A)

[8] B. Scholz, L. Ginzkey, and R. Abel: Evaluation of ambient noise measurements recorded during the NARSHA experiment 1987 (Preliminary data); 2 parts; FWG report no. 210, Sept. 1988. Data report. (A)

[9] B. Scholz, L. Ginzkey, and R. Abel: Evaluation of transmission loss measurements recorded during the NARSHA experiment 1987 (Preliminary data); 5 parts; FWG report no. 210, Sept. 1988. Data report. (A)

[10] FGAN: Sea surface backscatter measurements in the NARSHA experiment April/May 1987; Data results of the German 94 GHz Scatterometer; Report Forschungsinstitut für Hochfrequenzphysik, FGAN, 1988. Data report. (R)

Netherlands

[11] G.P. de Loor: NARSHA '87; Observation of the sea with the Dutch radars during NARSHA; Report FEL-TNO, 1988. (R+G)

Norway

[12] S.-E. Hamran and E. Aarholt: Sea surface measurements by the adaptive multifrequency radar system in the NARSHA German Bight experiment April/May 1987; Preliminary results; NTNF/PFM Technical Note TN-81/87; May 12, 1987. (R)

[13] S.-E. Hamran and E. Aarholt: Sea surface measurements by the adaptive multifrequency radar system in the NARSHA German Bight Experiment April/May 1987; Final report; NTNF/PFM Technical Note TN-82/87; Oct. 7, 1987. (R)

United Kingdom

[14] A.J. Randle: AVHRR products supplied to NARSHA experimenters by Space Department Royal Aerospace Establishment (UK); letter, Dec. 1988 (AVHRR images of 28 April, 6 and 7 May 1987). (G)

USA

[15] D.L. Schuler, G.L. Geernaert, and K.O. Hayes:
Vol. I: Airborne Ku-band radar backscatter measurements during NARSHA 87;
Vol. II: Airborne radar/radiometric measurements during individual overpasses over the acoustic range;
Report NRL NATO-186/88, 1988 (NATO CONFIDENTIAL) (R+G)

Supporting literature

Radar

[16] E.P.W. Attema et al.: Airborne and tower-based scatterometry campaigns; 14 papers in: 'Procs Third International Colloquium on Spectral Signatures in Remote Sensing', les Arcs (Fr), 16 - 20 Dec. 1985; ESA Publication SP-247, pp. 11-82.

[17] W.C. Keller, V. Wismann, and W. Alpers: Tower-based measurements of the ocean C-band radar backscattering cross section; J. Geophys. Res., vol. 94, no. C1, Jan. 15, 1989, pp. 924-930.

[18] G.P. de Loor: Slope modulation of the radar backscatter by sea waves; Report FEL-TNO no. FEL 1987-102; Report Netherlands Remote Sensing Board no. BCRS-88-05, Delft, April 1988.

[19] H. Masuko et al.: Measurement of microwave backscattering signatures of the ocean using X-band and Ku-band airborne scatterometers; J. Geophys. Res., vol. 91, no. C11, Nov. 15, 1986, pp. 13065-13083.

[20] L. Schröder et al.: The relationship between windvector and NRCS used to derive SEASAT-A satellite scatterometer winds (SASS-1 model); J. Geophys. Res., vol. 87, no. C5, April 30, 1982, pp. 3318-3336.

[21] H. Sittrop: X- and Ku-band radar backscatter characteristics of sea clutter; Procs URSI Commission II specialist meeting on 'Microwave scattering and emission from the earth' (editor: E. Schanda), Berne (Switzerland) 23 - 26 Sept. 1974, pp. 25-37.

[22] F.J. Wentz, S. Peteherych, and L.H. Thomas: A model function for ocean radar cross sections at 14.6 GHz (SASS-2 model); J. Geophys. Res., vol. 89, no. C3, May 20, 1984, pp. 3689-3704.

Environment

[23] R. Ezraty and M. Ollitrault: Estimation de la vitesse de frottement a la surface de la mer a partir de valeurs moyennes de vitesse du vent et des temperatures de l'air et de l'eau; report IFREMER. Brest (Fr), May 1, 1984.

Acoustics

[24] D.M. Farmer and D.D. Lemon: The influence of bubbles on ambient noise in the ocean at high wind speeds; J. Phys. Ocean., vol. 14, 1984, pp. 1762-1778.

[25] B.R. Kerman, Editor: Sea Surface Sound. Natural Mechanisms of Surface generated Noise in the Ocean. NATO ASI Series C 1989, (P.C. Wille and D. Geyer, pp. 295-308)

[26] B. Nützel et al.: A further investigation of acoustic scattering from the sea surface; FWG-report 1986-3; NUSC Technical Document 7685; 9 July 1986.

[27] P.C. Wille and D. Geyer: Measurements of the wind-dependent ambient noise variability in shallow water; J. Acoust. Soc. Am., vol. 75, no. 1, 1984, pp. 173-185.

List of Acronyms

ACRA	ACoustic RAnge
degr.	degree
DK	Denmark
DLR	Deutsche Forschungs- und Versuchsanstalt für Luft- und Raumfahrt e.V., former acronym: DFVLR
F	France
FEL TNO	Fysisch en Elektrisch Laboratorium TNO
FGAN-FHP	ForschungsGesellschaft für Angewandte Naturwissenschaften e.V. Forschungsinstitut für HochfrequenzPhysik
FPN	ForschungsPlattform NORDSEE
FWG	Forschungsanstalt der Bundeswehr für Wasserschall- und Geophysik
GE	Federal Republic of GErmany
GERDSM	Groupe Etudes et Recherches de Detection Sous Marine
N	Norway
NARSHA	NATO Acoustic and Remote Sensing SHallow Water - this experiment
NL	NetherLands
NNAG	NATO Naval Armament Group
NRCS	Normalized Radar Cross Section
NRL	Naval Research Laboratory
NTNF	Norges Teknisk- Naturvitenskapelige Forskninsgråd
RAE	Royal Aerospace Establishment
RSG	Research Study Group
SHIRA	SHIps RAdar
SLAR	Side Looking Airborne Radar
TI	Reynolds' stress
UK	United Kingdom
USA	United States of America
VV-pol.	transmitting and receiving of vertically polarized electromagnetic waves

Radar frequencies and central wave length

X-band:	8.0 - 12.5 GHz, 3 cm
K_u-band:	12.5 - 18.0 GHz, 2 cm
W-band:	56 - 100 GHz, 4 cm

List of the Members of AC/243 P.03 RSG.12

MEMBER	represented by
France	Direction des Recherches Etudes et Techniques SDR. - G. 32 26 Bd. Victor, F-75996 Paris Armees Mr H. Duchoussoy
Germany	Forschungsanstalt der Bundeswehr für Wasserschall- und Geophysik, Klausdorfer Weg 2-24, D-2300 Kiel 14 Mr. P.L. Lobemeier
Netherlands	Physics and Electronics Laboratory TNO P.O. Box 96864, 2509 JG The Hague until November 1989: Dr. G.P. de Loor (Chairman RSG.12) since November 1989: Dr. P. Hoogeboom (Chairman RSG.12)
Norway	Norwegian Defence Research Establishment Electronics Division P.O. Box 25 N-2007 Kjeller until 1988: Dr. K. Aksnes since November 1989: Dr. Tjerre Wahl
United Kingdom	Royal Aerospace Establishment Space Department, Q134 Bldg Farnborough, Hamshire GU14 6TD Dr. G. Keyte, Mr. Chris Brownsword
United States of America	Office fo Naval Research 800 N Quincy Street Arlington, Va. 22217 Mr. H. Dolezalek (now assigned to ONR European Office, London) Naval Research Laboratory Washingron Dc 20375 Dr. V.E. Noble Dr. D.L. Schuler (until November 1989 Secretary of RSG.12)
LIAISON	1. SACLANT Undersea Research Centre Viale San Bartholomeo (SP) La Spezia, Italy Dr. P.J. Minnett 2. HQ SACLANT Norfolk, VA 23511 represented by MILOC Secretary